Human Neutrophil Elastase Responsive Delivery from Poly(ethylene glycol) Hydrogels

Alex A. Aimetti,[†] Mark W. Tibbitt,[†] and Kristi S. Anseth[*,†,‡]

*Department of Chemical and Biological Engineering and the Howard Hughes Medical Institute,
University of Colorado, Boulder Colorado 80309*

Received January 22, 2009; Revised Manuscript Received March 16, 2009

A novel enzyme-responsive hydrogel drug delivery system was developed with the potential to treat inflammation locally. Human neutrophil elastase (HNE) is a serine protease secreted by neutrophils which are the first cells recruited to inflammatory sites. We exploited this cell-secreted enzyme as a biological cue for controlled release. HNE sensitive peptide linkers were immobilized within poly(ethylene glycol) hydrogels using photopolymerization techniques. The kinetics of the enzyme reaction within the gel was tailored by varying the amino acid residues present in the P1 and P1′ substrate positions (immediately adjacent to cleavage location). A novel FRET-based hydrogel platform was designed to characterize the accessibility of the substrate within the cross-linked, macroscopic hydrogel. Lastly, a diffusion-reaction mathematical model with Michaelis−Menten kinetics was developed to predict the overall release profile and captured the initial 80% of the experimentally observed release. The hydrogel platform presented shows highly controlled release kinetics with potential applications in cellular responsive drug delivery.

1. Introduction

A major goal in drug delivery is to control spatially and temporally the release of therapeutics in vivo. Localized and sustained drug delivery has the potential to enhance the therapeutic efficacy of treatment by minimizing systemic drug concentrations and the need for repeated drug administration.[1] More recently, efforts have been made to fabricate intelligent drug delivery systems that release therapeutics in response to physical or biological stimuli, such as temperature,[2,3] pH,[4−6] glucose,[7,8] or enzymes.[9−11] While these systems have provided great advancements in the area of controlled release, there remains a need for biomaterials to respond and adapt to cellular stimuli in the areas of drug delivery and tissue regeneration.

An emerging area of drug delivery focuses on localized, controlled release in recognition of a cellular response. For example, human bone morphogenetic protein-2 (BMP-2) has been entrapped within a 4-arm poly(ethylene glycol) (PEG) hydrogel cross-linked with matrix metalloproteinases (MMPs) sensitive peptides. Once implanted at defect sites in rat calvaria, cell-secreted MMPs were able to degrade the gel and liberate the encapsulated BMP-2, which promoted cell infiltration and led to remodeling of bony tissue.[12] In another approach, vascular endothelial growth factor (VEGF) was covalently attached to fibrin gels through thrombin cleavable substrates for wound healing applications.[13]

A similar approach can be taken to develop enzyme responsive biomaterials to achieve local drug delivery at sites of inflammation. Inflammation has been implicated in wound healing and many diseases such as diabetes,[14] rheumatoid arthritis,[15] and cancer.[16] During this biological response, immune cells infiltrate the site of infection/injury and secrete a variety of biomolecules in a protective attempt to remove the harmful stimuli. In specific, neutrophils are the first responding cells to these microenvironments.[17] Upon activation, neutrophils degranulate and release a variety of enzymes such as human neutrophil elastase (HNE). An elevated presence of this enzyme implies a highly specific biological event (disease or injury) is occurring, thus making HNE a desirable triggering molecule for local therapeutic delivery.[18] This serine protease has a specificity for small, uncharged amino acids, particularly alanine (A) and valine (V).[19] Synthetic peptides containing the sequence Ala-Ala-Pro-Val have been studied as HNE specific substrates[20] for drug delivery applications.[21] By incorporating a similar elastase sensitive peptide into a biomaterial, an increased local concentration of HNE at sites of degranulation can be used as a cellular cue to release an anti-inflammatory therapeutic.

In this contribution, we present and characterize a drug delivery platform with the potential to achieve HNE-triggered, controlled, and localized drug release from PEG hydrogels. Specifically, HNE-sensitive linkers were photopolymerized into PEG diacrylate (PEGDA) hydrogels as pendent groups as seen in Scheme 1. Upon the onset of an inflammatory response, HNE diffuses into the PEG hydrogels and cleaves its respective substrate liberating a therapeutic to the local environment. Research has shown that the amino acid positions directly adjacent to enzyme cleavage location (P1 and P1′) are important for varying proteolytic reaction rates.[22,23] This work examines the effect of point variations within the elastase substrate at specified locations on the cleavage kinetics and exploits these differences to obtain varying release profiles from the hydrogel. In addition, a Förster resonance energy transfer (FRET)-based hydrogel was developed to characterize the accessibility of the substrate to the enzyme within a cross-linked polymer network. Lastly, a diffusion-reaction model, taking into account both molecular diffusion and Michaelis−Menten kinetics, was developed to better understand the mechanisms dominating release from the HNE-responsive hydrogels.

---
* To whom correspondence should be addressed. E-mail: kristi.anseth@colorado.edu.
† Department of Chemical and Biological Engineering.
‡ Howard Hughes Medical Institute.

Scheme 1. Photopolymerization of PEGDA with an Acrylated HNE-Sensitive Substrate
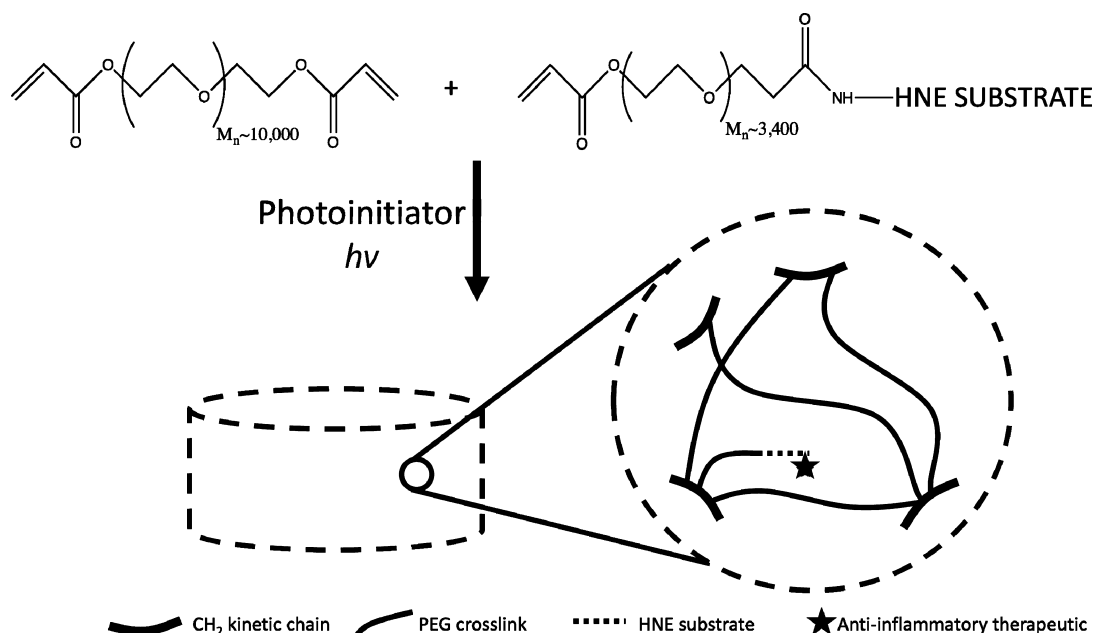
Table 1. HNE-Sensitive Peptides Synthesized Showing Point Variations in the P1 and P1′ Positions[a]

YAAP(P1) ↓ (P1′)GCG							
P1				P1′			
Ala	**Abu**	**Nva**	**Nle**	**Arg**	**Gln**	**Leu**	**Phe**
CH₃	CH₂ CH₂ CH₃	CH₂ CH₂ CH₂ CH₃	CH₂ CH₂ CH₂ CH₃	CH₂ CH₂ CH₂ NH C=NH NH₂	CH₂ CH₂ C=O NH₂	CH₂ CH—CH₃ CH₃	CH₂ (phenyl ring)

[a] Arrow indicates cleavage location. Unless otherwise noted, the default amino acid for the P1 position was Val and Gly for the P1′ position. Nonnative amino acid abbreviations represent Abu = aminobutyric acid, Nva = norvaline, and Nle = norleucine.
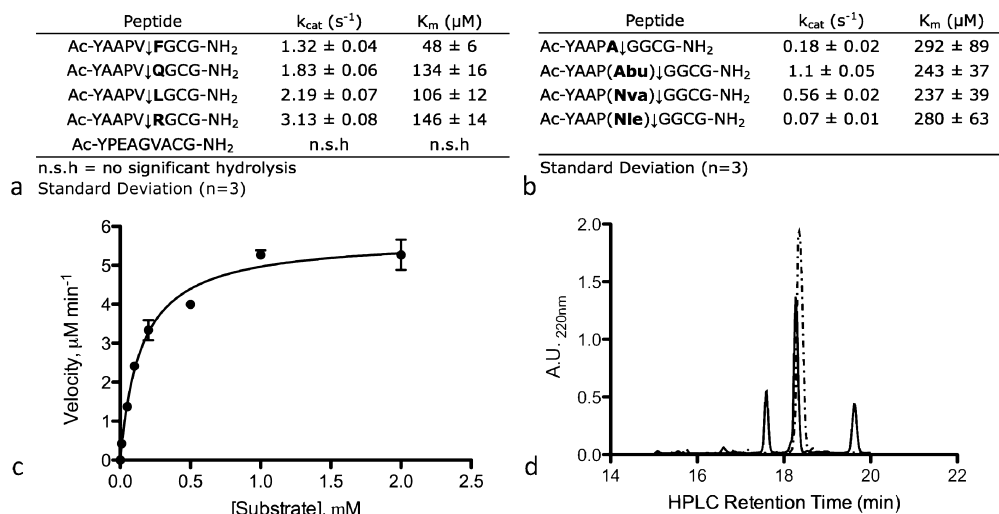
2. Experimental Section

Materials. Poly(ethylene glycol) (PEG, $M_n \sim 10000$) was obtained from Aldrich (St. Louis, MO). Monoacrylate-PEG-*N*-hydroxysuccinimide (APEG-NHS, $M_n \sim 3400$) was purchased from Laysan Bio, Inc. (Arab, AL). Fmoc-protected amino acids in their L-configuration as well as *O*-benzotriazole-N,N,N′,N′-tetramethyl-uronium-hexafluorophosphate (HBTU), 1-hydroxybenzotriazole hydrate (HOBt), and 2-(1*H*-7-azabenzotriazol-1-yl)-1,1,3,3-tetramethyl uronium hexafluorophosphate methanaminium (HATU) used for amino acid activation were obtained from Anaspec (San Jose, CA). MBHA Rink Amide resin was purchased from Novabiochem (La Jolla, CA). 5(6)-Carboxyrhodamine (ROX) and QXL 610 acid (QXL) were obtained from Anaspec. Fluorescamine was provided by Sigma-Aldrich (St. Louis, MO). Human neutrophil elastase (HNE) was supplied as a lyophilized powder from Innovative Research (Novi, MI).

Poly(ethylene glycol) Diacrylate (PEGDA10k) Synthesis. Linear PEGDA10k was synthesized similar to reported literature[24] by reacting PEG ($M_n \sim 10000$) with a 8 molar excess of acryloyl chloride in the presence of triethyleamine (TEA). The reaction was allowed to proceed overnight at room temperature protected from light. The acrylated PEG was filtered through a bed of alumina to remove the TEA−HCl complex. Toluene was then removed from the reaction mixture under rotary evaporation. To obtain pure PEGDA10k, the crude product was dissolved in methylene chloride and precipitated in cold diethyl ether. The purified product was then filtered and dried in vacuo at room temperature. The degree of acrylation was confirmed to be >90% by ¹H NMR (Supporting Information).

Peptide Synthesis. Peptide sequences (Table 1) were synthesized (Applied Biosystem 433A Peptide Synthesizer) using solid phase Fmoc chemistry on a MHBA Rink Amide Resin (~0.7 mmol/g resin substitution). Peptides were cleaved from their solid support using trifluoroacetic acid (TFA)/triisopropylsilane (TIS)/water (95/2.5/2.5 v/v) and allowed to react at room temperature for 2 h. The reaction was filtered and the filtrate precipitated and washed (3×) in chilled diethyl ether. Peptides were purified by semipreparative reversed phase HPLC (Waters Delta Prep 4000) using a 70 min linear (5−95%) gradient of acetonitrile in 0.1% trifluoroacetic acid. Peptide purity was confirmed by analytical reversed phase HPLC C18 column and matrix-assisted laser desorption ionization time-of-flight mass spectrometry (Applied Biosystem DE Voyager).

Kinetic Analysis of Substrate Degradation. Degradation kinetic parameters were determined using a fluorescamine fluorometric assay.[25] To measure accurately the concentrations of cleaved peptide fragments, the N-terminal amines of the HNE substrate peptides were capped with

Peptide	k_{cat} (s^{-1})	K_m (μM)
Ac-YAAPV↓**F**GCG-NH$_2$	1.32 ± 0.04	48 ± 6
Ac-YAAPV↓**Q**GCG-NH$_2$	1.83 ± 0.06	134 ± 16
Ac-YAAPV↓**L**GCG-NH$_2$	2.19 ± 0.07	106 ± 12
Ac-YAAPV↓**R**GCG-NH$_2$	3.13 ± 0.08	146 ± 14
Ac-YPEAGVACG-NH$_2$	n.s.h	n.s.h

n.s.h = no significant hydrolysis
a Standard Deviation (n=3)

Peptide	k_{cat} (s^{-1})	K_m (μM)
Ac-YAAP**A**↓GGCG-NH$_2$	0.18 ± 0.02	292 ± 89
Ac-YAAP(**Abu**)↓GGCG-NH$_2$	1.1 ± 0.05	243 ± 37
Ac-YAAP(**Nva**)↓GGCG-NH$_2$	0.56 ± 0.02	237 ± 39
Ac-YAAP(**Nle**)↓GGCG-NH$_2$	0.07 ± 0.01	280 ± 63

b Standard Deviation (n=3)

Figure 1. Solution phase hydrolysis of peptides by HNE. The values of k_{cat} and K_m for point variations in the P1′ (a) and P1 (b) substrate positions. Kinetic constants for the control substrate Ac-YAAPV↓GGCG were K_m = 160 ± 20 μM and k_{cat} = 2.68 ± 0.08 s^{-1}. Arrow indicates cleavage location. (c) Representative Michaelis−Menten plot. (d) Representative HPLC chromatogram showing pure peptide (dashed line) and peptide and HNE reaction mixture (solid lines).

acetic anhydride. Peptides were dissolved in reaction buffer (50 mM HEPES + 150 mM NaCl pH 7.4) at varying concentrations and HNE was added (30nM). The reaction mixture was sampled at 5-min intervals and allowed to further react with fluorescamine (2 mg/mL in acetonitrile) for determining the concentrations of cleaved peptides (fluorescence was detected at $\lambda_{excitation}$ = 380 nm, $\lambda_{emission}$ = 460 nm, Perkin-Elmer Wallac Victor[2] 1420 Multilabel Counter). Cleavage product concentration was determined using presynthesized peptide fragments as an external calibration. Michaelis−Menten enzyme kinetic analysis was performed and specificity constants (k_{cat}/K_m) were determined using nonlinear regression analysis (Graphpad Prism 5). Substrate cleavage site was confirmed by RP-HPLC analysis. The peptide fragments were isolated and analyzed with electrospray ionization mass spectrometry to determine the amino acid composition within the fragment.

Synthesis of HNE-Cleavable FRET Substrate. The peptide K(ROX)AAPV↓RGGGK(QXL) was synthesized as follows (where arrow indicates cleavage location). Fmoc-Lys(Mtt)-OH was allowed to couple to the resin (HATU/N,N′-diisopropylethylamine (DIPEA)) for 2 h. The resin was then treated with 1.8% TFA in dichloromethane for 30 s, repeated nine times[26] to selectively remove the Mtt protecting group on Lys. A ninhydrin test was performed to confirm the complete removal of the Mtt protecting group. QXL was then reacted to the deprotected ϵ-amino group (HATU/DIPEA) on Lys for 2 h. The resin was then thoroughly washed with DMF and placed on the ABI 433A Peptide Synthesizer for automated couplings. After peptide synthesis, Fmoc-K(Mtt)AAPVRGGGK(QXL)-resin was removed from the instrument and the Mtt group selectively deprotected as described above. ROX was reacted to the N-terminal Lys ϵ-amino group using HATU/DIPEA coupling chemistry. The terminal Fmoc group was manually removed (20% piperidine in DMF). Finally, the product was cleaved from the resin and purified as described above. The product was confirmed using MALDI-MS.

Visualization of HNE Activity in PEG Hydrogel. Acrylate-PEG-NHS (5 equiv) was reacted to the N-terminal amine of the FRET substrate in 0.1 M sodium phosphate buffer pH 8.0 for 4 h protected from light. The desired product (Acryl-PEG-K(ROX)-AAPV↓RGGGK(QXL)) was isolated using RP-HPLC and resulted in a lyophilized powder. Upon HNE dictated cleavage, the QXL quencher is able to diffuse away, leaving fluorescent ROX that provides spatial evidence of HNE activity within our gels. FRET hydrogels were formed from a precursor solution of 10 wt % PEGDA10k in phosphate buffer (PBS), 0.025 wt % of the photoinitiator 2-hydroxy-1-[4-(hydroxyethoxy)phenyl]-2-methyl-1-propanone (I-2959, Ciba-Geigy), and 4 mM acryl-PEG-K(ROX)AAPVRGGGK(QXL), exposed to 365 nm ultraviolet

light for 10 min. Gels were treated with 1 μM HNE and 3-dimensional fluorescence image stacks, spanning the thickness of the hydrogel, were captured at predetermined time points using confocal microscopy (Zeiss Pascal LSM 5). ROX was excited using a 543 nm helium−neon laser and fluorescence was collected using a 560 nm long pass filter.

HNE Dictated Release From PEG Hydrogel. Two HNE substrates analyzed using the solution phase assay were further studied in an immobilized hydrogel system. Peptides AAPV↓RGMG and AAP(Nva)↓GGMG were acrylated with conjugation to APEG-NHS and purified as described previously. Methionine residues were substituted for cysteine residues, as used previously, to prevent thiol−acrylate reaction during photopolymerization. Hydrogels were formed via free radical photopolymerization from the macromer solution containing 10 wt % PEGDA10k, 5 mM APEG-peptide, and 0.025 wt % I-2959 under standard conditions described previously. Cylindrical disks (diameter = 5 mm, thickness = 600 μm) were formed using a biopsy punch. Roughly 85% of the APEG-peptide was incorporated during the photopolymerization, which is comparable to previous literature using similar reaction conditions.[27] This was determined by swelling the gels in buffer for 24 h and exposing the supernatant to HNE (1 μM). The reaction was allowed to proceed for 2 h to ensure complete substrate cleavage. Fluorescamine was added and the amount of peptide in the buffer solution was determined using an external calibration with the peptide fragment. Gels (n = 3) were then transferred to 100 μL of fresh HEPES buffer and 1 μM HNE was added. At predetermined time points, samples were analyzed for peptide fragment release using fluorescamine. Buffer and enzyme was replenished at each time point.

3. Results and Discussion

3.1. Solution Phase Enzyme Kinetic Analysis of HNE Substrates. To tailor drug delivery in enzyme responsive materials, it is important to characterize the kinetic rate at which the enzyme is breaking down its respective substrate. HNE substrates were synthesized with point variations in the P1 and P1′ amino acid positions with the goal of manipulating the reaction kinetics. Rational design was used to vary residues within these locations. Previous literature reports that HNE specificity for its substrate depends greatly on S′−P′ interactions.[28] Therefore, we examined a charged amino acid (Arg), a neutral, hydrophilic residue (Gln), a hydrophobic, aliphatic amino acid (Leu), and a hydrophobic, aromatic residue (Phe) in the P1′ location (Table 1). Figure 1a shows that hydrophobic
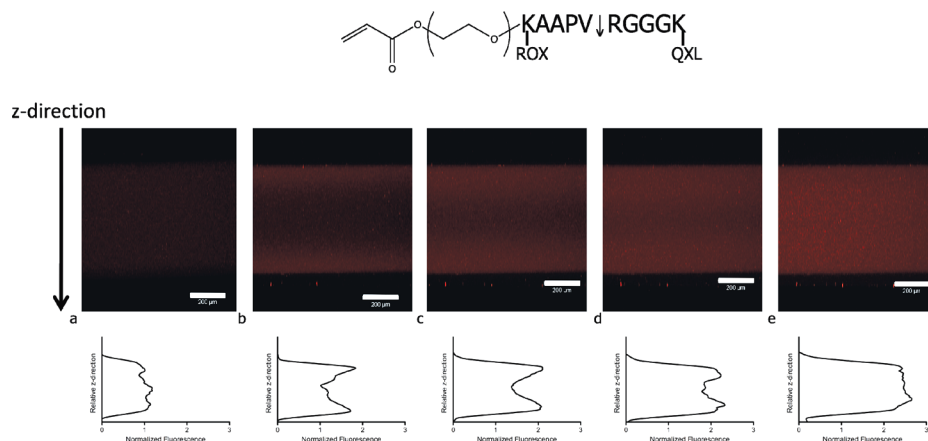
Figure 2. Spatial HNE activity progression at (a) 0, (b) 1, (c) 3, (d) 5, and (e) 10 min throughout the thickness of a hydrogel. Scale bars = 200 μm. Graphs depict quantitative fluorescence analysis as a function of a representative hydrogel thickness.

interactions play a dominant role in protein-peptide binding ($\sim K_m$) similar to previous reports.[28] K_m values ranged from 150 μM (Arg in P1′ position) to 50 μM (Phe in P1′ position). An increase in substrate hydrophobicity led to a decrease in K_m values indicating enhanced protein-peptide affinity. Incorporation of an Arg residue enhanced the catalytic efficiency similar to studies by Korkmaz et al.[29] An $\sim$2.5-fold difference was seen in k_{cat} values ranging from 3.1 to 1.3 s^{-1} for Arg and Phe P1′ containing peptides, respectively. Electrostatic interactions could contribute to this result based on the surface charge distribution on HNE, as HNE exhibits a slightly negative surface charge in close proximity to the catalytic site.[29] In addition, a scrambled peptide exhibited resistance to HNE cleavage showing specificity of the other substrates.

In further attempts to tailor the kinetic rate of HNE-mediated substrate degradation, we studied the incorporation of non-natural amino acids in the P1 position (Table 1). HNE is known to prefer short, aliphatic amino acids in the P1 site.[30,31] The S1 pocket of HNE is shallow compared to its serine protease counterparts due to the presence of Val-190 and Val-216 residues.[32] Therefore, we investigated non-native residues whose side chains differ by varying numbers of methylene groups. Figure 1b indicates there is a preferred size of the P1 side chain length (Abu with ethyl group) for effective HNE substrate degradation. HNE degraded substrates containing a short P1 amino acid side chain (Ala) and longer P1 residue side chains (Nle) at a rate constant of 0.18 and 0.07 s^{-1}, respectively. A maximum k_{cat} constant (1.1 s^{-1}) for P1 amino acid variations was found with an Abu (ethyl side chain) containing peptide. The Michaelis constant remained similar (240−290 μM) for the P1 varied substrates indicating comparable protein−peptide affinity. These results demonstrate that the point variations on HNE substrate peptides affect the catalytic activity of HNE. Figure 1c contains a representative Michaelis−Menten plot (substrate: Ac-YAAPVRGCG) illustrating the enzyme kinetics of HNE dictated substrate cleavage. Further, HPLC was used to separate the peptide fragments and nondegraded peptide within an HNE-peptide containing reaction mixture. Nondegraded peptide and two peptide fragment peaks are observed in Figure 1d corresponding to Ac-YAAPVRGCG and Ac-YAAPV/RGCG, respectively (MALDI spectra can be found in Supporting Information).

In conclusion, it was possible to alter the rates of HNE-dictated cleavage by simply varying a single amino acid residue in specific locations along the substrate sequence. The results presented herein provide the foundation for achieving tailorable HNE-responsive drug delivery from PEG hydrogels.

3.2. Visualizing HNE Activity in a PEG Hydrogel Using FRET. When designing enzyme responsive delivery platforms, it is critical to understand the accessibility of the substrate to the enzyme.[33] PEGDA photopolymerized hydrogels are highly cross-linked, three-dimensional polymeric networks. This structure impedes (and at some molecular weight cut off denies) the diffusion of proteins through the hydrogel network. Other than pathological reasons, HNE was chosen as a triggering molecule due its relative small size ($\sim$29.5 kDa) and ability to penetrate the hydrogel.[34] By incorporating a FRET based HNE substrate within the hydrogel, HNE spatial activity could be visualized using confocal microscopy. We developed a FRET hydrogel system where a fluorophore/quencher HNE substrate (K(ROX)AAPV↓RGGGK(QXL)) was photopolymerized within a PEG hydrogel. Upon HNE dictated cleavage, the QXL quencher was able to diffuse out of the gel allowing for the detection of the ROX fluorophore. Figure 2 shows the enzyme cleavage front as a function of space and time. Figure 2a shows a uniform fluorescence profile over the thickness of the hydrogel. Over time, an increase in normalized fluorescence was initially observed at the gel edges and propagated inward toward the center. At t = 10 min, increased uniform fluorescence ($\sim$2.5 times the initial value) was observed through the z-direction of the gel. Our results indicate that HNE is able to access the center of the hydrogel within a reasonable time scale (minutes), but both mass transfer and kinetics are important in dictating the overall release profile.

3.3. Modeling Enzymatic Cleavage and Release from PEG Hydrogel. To predict release profiles from this system, a reaction−diffusion model was developed, based on similar approaches in the literature.[35,36] Briefly, substrate cleavage was assumed to be governed by Michaelis−Menten kinetics (Figure 1) with a spatially heterogeneous HNE concentration dictated by HNE's diffusion into the gel as well as its measured half-life. The cleaved product then diffused out of the hydrogel and the product residing in the supernatant at each time point was measured.

The diffusion of HNE was modeled by unidirectional, Fickian diffusion through the vertical axis of the hydrogel such that

$$\frac{\partial [\text{HNE}](z, t)}{\partial t} = D_{\text{E}} \frac{\partial^2 [\text{HNE}](z, t)}{\partial z^2} \tag{1}$$

where D_{E} is the diffusion coefficient of the enzyme in the gel and [HNE] is the concentration of enzyme at a given point in space and time. The diffusion coefficient of HNE ($D_{\text{E}} = 5 \times 10^{-7}$ cm^2 s^{-1}) was estimated from studies with a similar size

protein (carbonic anhydrase) diffusing through a hydrogel with similar gel chemistry.[34] At the surface ($x = 0$) of the hydrogel, a boundary condition was set as $[HNE] = [HNE]_0$, where $[HNE]_0$ is the concentration of enzyme in solution. At the center of the gel, the symmetry boundary condition was employed. Solving eq 1 and the corresponding boundary conditions leads to the solution

$$[HNE](z,t) = [HNE]_0 \left(1 - \frac{4}{\pi} \sum_{n=0}^{\infty} \frac{(-1)^n}{2n+1} \times \right.$$
$$\left. \exp\left[-D_E(2n+1)^2 \frac{\pi^2 t}{4h^2} \right] \cos\left[\frac{(2n+1)\pi z}{2h} \right] \right) \quad (2)$$

where h is the half-thickness of the gel ($h = 300 \ \mu$m). When the spatial profile of enzyme concentration from eq 2 was used and assuming that the cleavage of substrate follows Michaelis–Menten kinetics, the amount of substrate cleaved and product formed at each point in the gel is predicted by the following kinetic equations

$$-\frac{\partial[S](z,t)}{\partial t} = \frac{\partial[P](z,t)}{\partial t} = [HNE](z,t)k_{cat}\frac{[S]}{K_m + [S]} \quad (3)$$

where $[S]$ is the concentration of substrate, k_{cat} is the kinetic constant for formation of product for the given HNE–substrate pair, as measured in solution, K_m is the Michaelis constant for the given HNE-substrate pair as measured in solution, and $[P]$ is the concentration of cleaved product. The diffusion of the cleaved product is also modeled by unidirectional, Fickian diffusion through the vertical axis of the gel such that

$$\frac{\partial[P](z,t)}{\partial t} = D_P \frac{\partial^2[P](z,t)}{\partial z^2} \quad (4)$$

where D_P is the diffusion coefficient of the cleaved product in the gel. The product diffusion coefficient in dilute solutions was first approximated using the Stokes–Einstein equation (eq 5).

$$D_0 = \frac{k_B T}{6\pi \eta r_s} \quad (5)$$

When a correlation developed by Lustig et al.[37] was used, D_P in a cross-linked hydrogel was calculated to be 4.0×10^{-6} cm²/s. This relationship can be used to approximate the diffusion of various molecules, such as small molecules or globular proteins, because it takes into account the hydrodynamic radius of the solute, the mesh size of the cross-linked network, and the volume degree of swelling for the gel. Product diffusion was modeled numerically using a second-order, centered difference approximation of the second-derivate.

Figure 3 shows the experimentally measured and predicted release profiles using two HNE substrates (AAPVRGMG, AAP(Nva)GGMG) and varying concentrations of HNE. The two substrates examined were chosen based on the varying catalytic rates determined previously. Figure 3a shows varying release rates as a function of HNE concentration with the incorporation of substrate AAPVRGMG. Exogenously adding 1 μM HNE resulted in complete peptide release about 1 h, whereas 100 nM HNE dictated release occurred over 6 h. Figure 3b illustrates peptide release profiles from incorporated substrates with varying enzyme kinetic rates. For all systems where the reaction rate was increased (increased [HNE] or k_{cat}) there was an increasing linear release response at $t \geq 0$. However, when the rate of reaction was decreased (decreased [HNE] or k_{cat}), the data depicts an initial delay in release, which is most likely
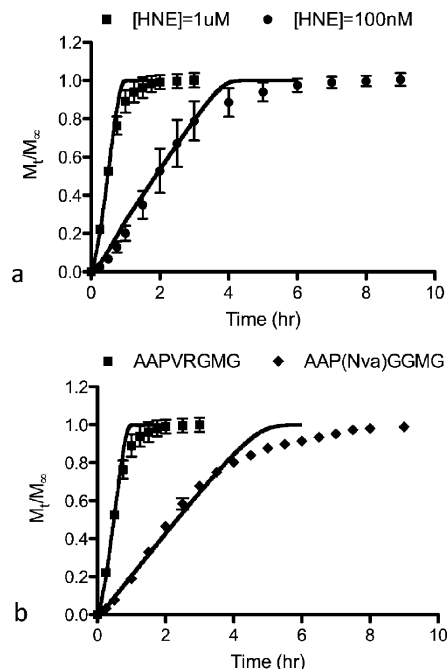
Figure 3. Peptide release profiles as a function of time from hydrogel in the presence of (a) varying HNE concentrations and (b) varying HNE substrates. Solid lines indicate diffusion-reaction model results. Error bars indicate standard deviation ($n = 3$).

attributed to diffusion limitations. The model agrees with the experimental values up to 80% release. At this point, the model and the experimental results deviate, which is likely due to the complexity of the system at later time points. As substrate is being converted to product, free carboxylic acids are present forming a more polyelectrolyte hydrogel. Upon HNE cleavage, the peptide fragments diffusing out of the gel (product) are cationic. Electrostatic attraction between the gel and the product could potentially decrease the diffusion rate out the gel.[38] This phenomenon would result in the mathematical model over predicting the rate of release as observed.

These results focus on the ability to tune release from the developed platform. To further enhance the value of the system, anti-inflammatory therapeutics can be covalently attached to the released peptide fragment through various bioconjugation techniques. Specifically, small molecule drugs such as lisofylline,[39] ketoprofen,[40] and D-penicillamine[41] are of interest due to their function and ability to incorporate onto the HNE substrate.

4. Conclusion

An enzyme responsive PEG hydrogel platform was developed to achieve HNE triggered release to the local environment. The rate of enzyme reaction (substrate degradation) can be tailored by incorporation and/or substitution of different amino acids in specific locations of the substrate. A novel FRET-based hydrogel platform was fabricated to image enzyme activity throughout the thickness of the macroscopic gel. The release from the hydrogel can be modeled using a diffusion-reaction model with molecular diffusion and Michaelis–Menten kinetics. This work fully characterized the drug delivery platform and exhibited the ability to achieve local, controlled release in the presence of HNE. In addition, this system could be further expanded to target other cell-secreted enzymes to target different stages of inflammation. Further studies involving conjugation of an active therapeutic to the substrate are necessary to validate the system.

Supporting Information Available. ^{1}H NMR of PEGDA10k, representative MALDI spectra, and digital image of the PEG-*co*-peptide hydrogel. This material is available free of charge via the Internet at http://pubs.acs.org.

References and Notes

(1) Langer, R. *Science* **1990**, *249* (4976), 1527–1533.
(2) van Bommel, K. J.; Stuart, M. C.; Feringa, B. L.; van Esch, J. *Org. Biomol. Chem.* **2005**, *3* (16), 2917–2920.
(3) Afrassiabi, A.; Hoffman, A. S.; Cadwell, L. A. *J. Membr. Sci.* **1987**, *33* (2), 191–200.
(4) Dong, L. C.; Hoffman, A. S. *J. Controlled Release* **1991**, *15* (2), 141–152.
(5) Gillies, E. R.; Goodwin, A. P.; Frechet, J. M. *Bioconjugate Chem.* **2004**, *15* (6), 1254–1263.
(6) Aspden, T. J.; Mason, J. D. T.; Jones, N. S.; Lowe, J.; Skaugrud, O.; Illum, L. *J. Pharm. Sci.* **1997**, *86* (4), 509–513.
(7) Duncan, R. *Nat. Rev. Drug Discovery* **2003**, *2* (5), 347–360.
(8) Rajangam, K.; Behanna, H. A.; Hui, M. J.; Han, X.; Hulvat, J. F.; Lomasney, J. W.; Stupp, S. I. *Nano Lett.* **2006**, *6* (9), 2086–2090.
(9) Law, B.; Weissleder, R.; Tung, C. H. *Biomacromolecules* **2006**, *7* (4), 1261–1265.
(10) Lee, M. R.; Baek, K. H.; Jin, H. J.; Jung, Y. G.; Shin, I. *Angew. Chem., Int. Ed.* **2004**, *43* (13), 1675–1678.
(11) Thornton, P. D.; McConnell, G.; Ulijn, R. V. *Chem. Commun.* **2005**, (47), 5913–5915.
(12) Lutolf, M. R.; Weber, F. E.; Schmoekel, H. G.; Schense, J. C.; Kohler, T.; Muller, R.; Hubbell, J. A. *Nat. Biotechnol.* **2003**, *21* (5), 513–518.
(13) Sakiyama-Elbert, S. E.; Panitch, A.; Hubbell, J. A. *FASEB J.* **2001**, *15* (7), 1300–1302.
(14) Koulmanda, M.; Bhasin, M.; Hoffman, L.; Fan, Z.; Qipo, A.; Shi, H.; Bonner-Weir, S.; Putheti, P.; Degauque, N.; Libermann, T. A.; Auchincloss, H., Jr.; Flier, J. S.; Strom, T. B. *Proc. Natl. Acad. Sci. U.S.A.* **2008**, *105* (42), 16242–16247.
(15) Choy, E. H. S.; Panayi, G. S. *N. Engl. J. Med.* **2001**, *344* (12), 907–916.
(16) Schafer, M.; Werner, S. *Nat. Rev. Mol. Cell Biol.* **2008**, *9* (8), 628–638.
(17) Lokuta, M. A.; Nuzzi, P. A.; Huttenlocher, A. *Proc. Natl. Acad. Sci. U.S.A.* **2003**, *100* (7), 4006–4011.
(18) Owen, C. A.; Campbell, E. J. *J. Leukocyte Biol.* **1999**, *65* (2), 137–150.
(19) Meers, P. *Adv. Drug Delivery Rev.* **2001**, *53* (3), 265–272.
(20) Wiesner, O.; Litwiller, R. D.; Hummel, A. M.; Viss, M. A.; McDonald, C. J.; Jenne, D. E.; Fass, D. N.; Specks, U. *FEBS Lett.* **2005**, *579* (24), 5305–5312.
(21) Pak, C. C.; Erukulla, R. K.; Ahl, P. L.; Janoff, A. S.; Meers, P. *Biochim. Biophys. Acta* **1999**, *1419* (2), 111–126.
(22) Lesner, A.; Kupryszewski, G.; Rolka, K. *Biochem. Biophys. Res. Commun.* **2001**, *285* (5), 1350–1353.
(23) Mucha, A.; Cuniasse, P.; Kannan, R.; Beau, F.; Yiotakis, A.; Basset, P.; Dive, V. *J. Biol. Chem.* **1998**, *273* (5), 2763–2768.
(24) Cruise, G. M.; Scharp, D. S.; Hubbell, J. A. *Biomaterials* **1998**, *19* (14), 1287–1294.
(25) Lauer-Fields, J. L.; Tuzinski, K. A.; Shimokawa, K.; Nagase, H.; Fields, G. B. *J. Biol. Chem.* **2000**, *275* (18), 13282–13290.
(26) Li, D.; Elbert, D. L. *J. Pept. Res.* **2002**, *60* (5), 300–303.
(27) Hern, D. L.; Hubbell, J. A. *J. Biomed. Mater. Res., Part A* **1998**, *39* (2), 266–276.
(28) Korkmaz, B.; Attucci, S.; Moreau, T.; Godat, E.; Juliano, L.; Gauthier, F. *Am. J. Respir. Cell Mol. Biol.* **2004**, *30* (6]?>),]?>), 801–807.
(29) Korkmaz, B.; Hajjar, E.; Kalupov, T.; Reuter, N.; Brillard-Bourdet, M.; Moreau, T.; Juliano, L.; Gauthier, F. *J. Biol. Chem.* **2007**, *282* (3), 1989–1997.
(30) Rao, N. V.; Wehner, N. G.; Marshall, B. C.; Gray, W. R.; Gray, B. H.; Hoidal, J. R. *J. Biol. Chem.* **1991**, *266* (15), 9540–9548.
(31) Kao, R. C.; Wehner, N. G.; Skubitz, K. M.; Gray, B. H.; Hoidal, J. R. *J. Clin. Invest.* **1988**, *82* (6), 1963–1973.
(32) Navia, M. A.; McKeever, B. M.; Springer, J. P.; Lin, T. Y.; Williams, H. R.; Fluder, E. M.; Dorn, C. P.; Hoogsteen, K. *Proc. Natl. Acad. Sci. U.S.A.* **1989**, *86* (1), 7–11.
(33) Ulijn, R. V. *J. Mater. Chem.* **2006**, *16* (23), 2217–2225.
(34) Weber, L. M.; Lopez, C. G.; Anseth, K. S. *J. Biomed. Mater. Res., Part A* **2008**, DOI: 10.1002/jbm.a.32134.
(35) Ehrbar, M.; Metters, A.; Zammaretti, P.; Hubbell, J. A.; Zisch, A. H. *J. Controlled Release* **2005**, *101* (1−3), 93–109.
(36) Tzafriri, A. R.; Bercovier, M.; Parnas, H. *Biophys. J.* **2002**, *83* (2), 776–793.
(37) Lustig, S. R.; Peppas, N. A. *J. Appl. Polym. Sci.* **1988**, *36* (4), 735–747.
(38) Chen, S. B. *J. Colloid Interface Sci.* **1998**, *205* (2), 354–364.
(39) Yang, Z. D.; Chen, M.; Wu, R.; McDuffie, M.; Nadler, J. L. *Diabetologia* **2002**, *45* (9), 1307–1314.
(40) Ricci, M.; Blasi, P.; Giovagnoli, S.; Rossi, C.; Macchiarulo, G.; Luca, G.; Basta, G.; Calafiore, R. *J. Controlled Release* **2005**, *107* (3), 395–407.
(41) Cui, Z. R.; Lockman, P. R.; Atwood, C. S.; Hsu, C. H.; Gupte, A.; Allen, D. D.; Mumper, R. J. *Eur. J. Pharm. Biopharm.* **2005**, *59* (2), 263–272.

BM9000926